Synthesis and Superconductivity of Electrochemically Grown Single-Crystal Aluminum Nanowires

Meenakshi Singh,[†,‡] Jian Wang,[†,‡] Mingliang Tian,[†,‡] Qi Zhang,[†] Alexis Pereira,[⊥] Nitesh Kumar,[†,‡] Thomas E. Mallouk,[†,‡,§] and Moses H. W. Chan*,[†,‡]

[†]*Center for Nanoscale Science*, [‡]*Department of Physics*, [§]*Department of Chemistry, Pennsylvania State University, University Park, Pennsylvania 16802, and* [⊥]*University of Puerto Rico, Cayey, PR 00736*

Superconducting systems with one or more physical dimensions smaller than the phase coherence length ($\xi(T)$) exhibit behavior different from bulk superconductors.[1] These quasi-two-dimensional (2D) or one-dimensional (1D) systems are a subject of great interest both for fundamental physics and potential technological applications.

Aluminum nanowires (ANW) have been a favorite candidate for studying superconductivity in the quasi-1D regime for several reasons. The long $\xi(T)$ of bulk Al, at 1600 nm, makes it easier to access the quasi 1D regime. Al has a thin, and stable oxide surface layer, protecting it from uncontrolled oxidation. These factors make ANW ideal candidates for making four probe-transport measurements on single nanowires, enabling experiments exploring phenomena like quantum phase slips and the antiproximity effect in quasi 1D systems. Tunneling experiments to explore superconductivity in 1D are also possible on ANW since the oxide surface layer on these wires is highly insulating. Lastly, ANWs are possible candidates for electronic circuits in future nanodevices.

Most experimental studies on ANW[2−5] and other nanowires[5−9] have been carried out on polycrystalline or amorphous samples. It is difficult to separate the effects of morphology and disorder from intrinsic quasi 1D and 2D physics from these studies. To enhance our understanding of the physics of quasi 1D systems, it is important to study single-crystal nanowires, where the effect of morphology and disorder can be mostly eliminated. The synthesis of

ANW has been done using injection,[10] electron beam lithography (EBL),[11] and electrochemistry using molten salts.[12] Unfortunately, none of these methods yields single-crystal nanowires. In this paper, a simple, inexpensive, and flexible technique to synthesize arrays of single-crystal ANW of controllable diameters using template-based electrodeposition is reported. Four-probe electronic transport measurements made on 70 nm diameter ANWs are also reported.

Al, being very active, has to be deposited in a dry atmosphere from an anhydrous electrolyte. In this study, the electrolytic bath was composed of 6 M $AlCl_3$ and 0.2 M $LiAlH_4$ in tetrahydrofuran (THF). The electrodeposition was carried out inside a glovebox (Vacuum Atmospheres Company) in a 99.999% pure nitrogen atmosphere, with less than 1 ppm moisture, and oxygen. The templates used were anodic aluminum oxide (AAO) membranes. Fifty and eighty nanometer pore diameter membranes were prepared using a constant voltage anodization process described elsewhere.[13] The membranes were coated on one side with a layer (150 and 200 nm respectively) of thermally evaporated Ag. This Ag layer acts as a cathode. A Pt anode was used and Al was deposited at a constant current density of 1.3−2.5 mA cm^{-2} for 45−60 min.

X-ray diffraction (XRD) was performed on ANW arrays embedded in the AAO membrane using Cu Kα radiation (Philips PW3040). Figure 1 shows the XRD pattern from a 50 nm ANW array. The peaks at 44.7 and 99.0° correspond to the {220} and {440} planes of face-centered cubic (FCC) Al. XRD patterns from ANW arrays of diameters 80 and 200 nm show the same reflections. This shows that the ANW are crystalline with [110] as the preferred growth direction.

To obtain freestanding ANW, the Ag film on the back of the AAO membrane has to be removed and the membrane dissolved. To prevent the HNO_3 used for Ag film removal from damaging the ANW, we deposited Au into the AAO membranes for 2 min before the Al electrodeposition. The Ag film could thus be etched away with concentrated HNO_3. After removal of the Ag film, the AAO membrane was dissolved in a solution containing 6% H_3PO_4 (by weight) and 1.8% CrO_3 (by weight), heated to 60°, for several hours. The ANWs suspended in the solution obtained were cleaned by washing several times with isopropyl alcohol (IPA), alternating with centrifugal separation.

*Corresponding author.
(1) Arutyunov, K.; Golubev, D.; Zaikin, A. *Phys. Rep.* **2008**, *464*, 1.
(2) Santhanam, P.; Chi, C. C.; Wind, S. J.; Brady, M. J.; Bucchignano, J. J. *Phys. Rev. Lett.* **1991**, *66*, 2254.
(3) Zgirski, M.; Riikonen, K. P.; Touboltsev, V.; Arutyunov, K. *Nano Lett.* **2005**, *5*, 1029.
(4) Altomare, F.; Chang, A. M.; Melloch, M. R.; Hong, Y.; Tu, C. W. *Phys. Rev. Lett.* **2006**, *97*, 017001.
(5) Altomare, F.; Chang, A. M.; Melloch, M. R.; Hong, Y.; Tu, C. W. *Appl. Phys. Lett.* **2005**, *86*, 172501.
(6) Rogachev, A.; Bollinger, A. T.; Bezryadin, A. *Phys. Rev. Lett.* **2005**, *94*, 017004.
(7) Bezryadin, A.; Lau, C.; Tinkham, M. *Nature* **2000**, *404*, 971.
(8) Geim, A.; Dubonos, S.; Lok, J.; Henini, M.; Maan, J. *Nature* **1998**, *396*, 144.
(9) Giordano, N.; Schuler, E. *Phys. Rev. B* **1990**, *41*, 11822.

(10) Huber, C.; Huber, T.; Sadoqi, M.; Lubin, J.; Manalis, S.; Prater, C. *Science* **1994**, *263*, 800.
(11) Tamada, H.; Doumuki, T.; Yamaguchi, T.; Matsumoto, S. *Opt. Lett.* **1997**, *22*, 419.
(12) Liao, Q.; Pitner, W.; Stewart, G.; Hussey, C.; Stafford, G. *J. Electrochem. Soc.* **1997**, *144*, 936.
(13) Tian, M.; Xu, S.; Wang, J.; Kumar, N.; Wertz, E.; Li, Q.; Campbell, P.; Chan, M.; Mallouk, T. *Nano Lett.* **2005**, *5*, 697.
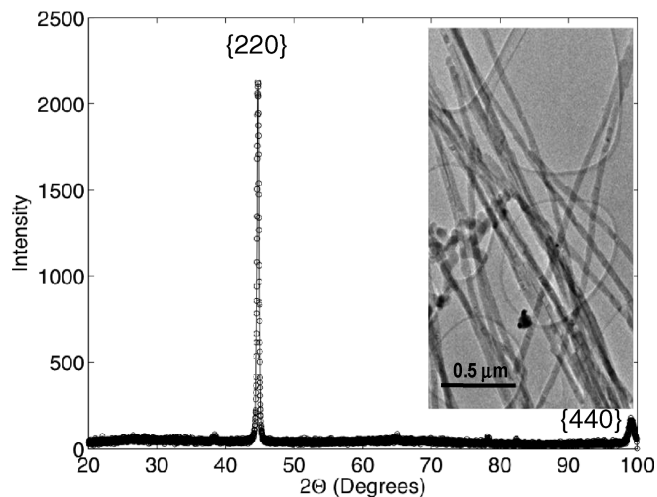
Figure 1. XRD spectrum of 50 nm ANW array embedded in an AAO membrane. The peaks at 44.7 and 99.0° correspond to the {220} and {440} planes, respectively. The inset shows a TEM image of 50 nm ANW after being released from the membrane and dispersed on a carbon-coated copper grid.
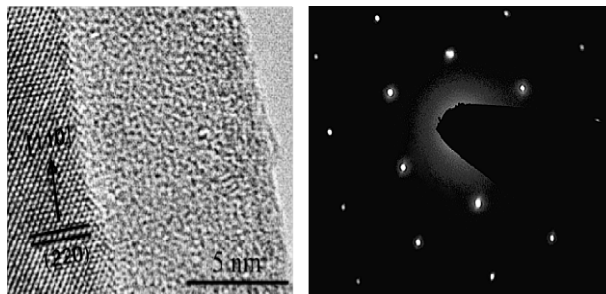

Figure 2. (Left) HRTEM image of a 50 nm ANW. The 10 nm thick amorphous oxidation layer can be seen. (Right) SAED pattern from the wire. The diffraction pattern with hexagonal symmetry corresponds to the pattern from FCC aluminum with $[\bar{1}11]$ as the beam direction.

Clean ANWs in IPA were dispersed on a Cu grid for structural characterization using transmission electron microscopy (TEM, Philips EM-420T), high-resolution transmission electron microscopy (HRTEM) and selected area electron diffraction (SAED) in a F-2010 field-emission TEM. An HRTEM image of a 50 nm thick wire is shown in the left panel of Figure 2. The HRTEM image shows an amorphous oxidation layer ~10 nm in thickness on the surface of the wire. The oxidation layer makes the diameter of the nominally 50 nm nanowire effectively 30 nm. The thickness of the oxidation layer decreases with increasing nanowire diameter and is stable with time. The oxidation layer on the nanowires is significantly thicker than the oxidation layer on amorphous aluminum nanowires.[5] This may be caused by the aggressive etching procedure employed to release the ANW from the alumina membrane. The crystallinity of the wire, as shown by the XRD pattern, is also confirmed by the HRTEM. The SAED pattern (right panel of Figure 2) has hexagonal symmetry. For FCC ANW with [110] as the growth direction and $[\bar{1}11]$ as the beam direction, this is the pattern that would be expected. The needle inserted to block the direct beam obscures the sixth spot in the inner hexagon. The TEM and XRD
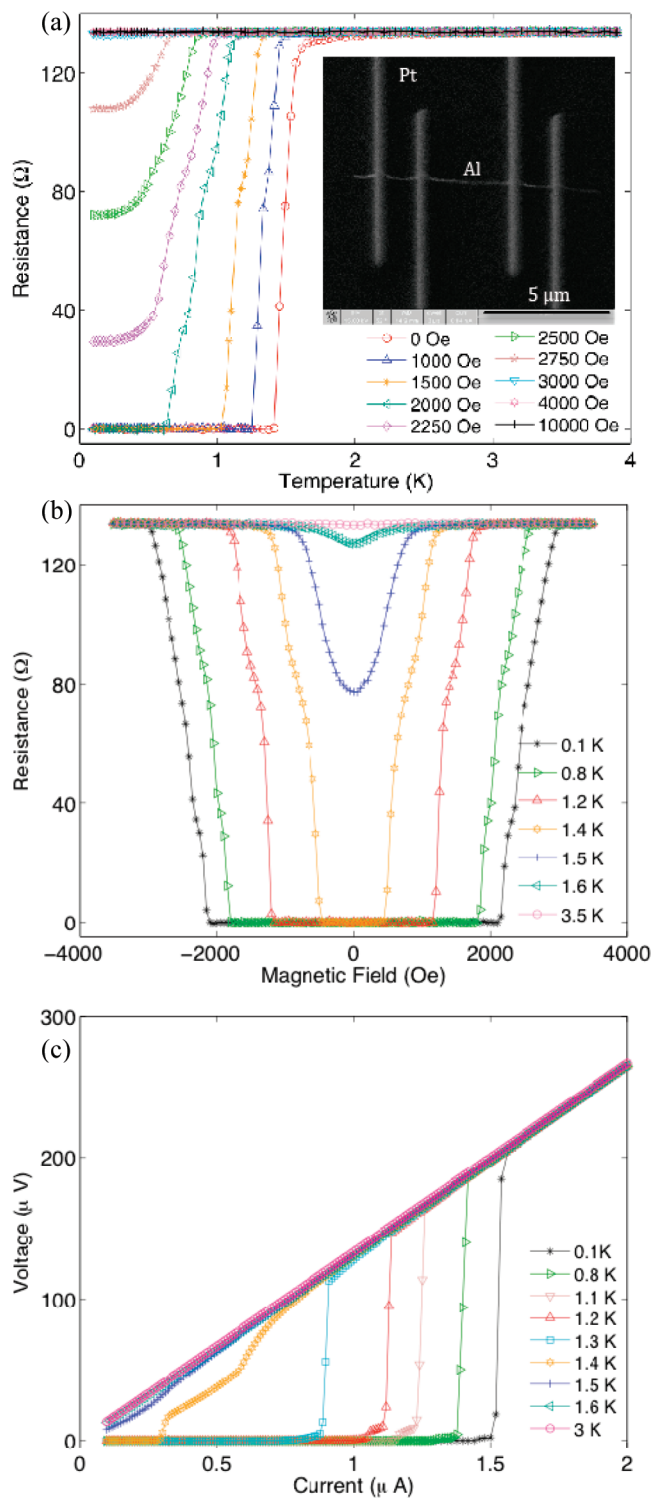

Figure 3. (a) Resistance as a function of temperature for a 70 nm ANW at different magnetic fields at an excitation current of 100 nA. $T_c = 1.7\,K$. The inset shows an SEM image of a 30 nm diameter ANW with four Pt electrodes. (b) Resistance as a function of magnetic field at different temperatures. The critical magnetic field at the 0.1 K is ~3000 Oe. (c) Voltage as a function of excitation current. The critical current at 0.1 K is 1.5 μA.

results for 80 nm ANW are similar to that shown in Figure 1 for the 50 nm wires.

Transport measurements were performed on individual nanowires using a physical properties measurement system (Quantum Design Inc.), equipped with a Dilution Refrigerator (DR) and a superconducting magnet.

To make 4-electrode measurements on the single ANW, a drop of the suspension of ANW in IPA was dispersed on a Si_3N_4/Si wafer. A dual-beam FEI Quanta 200 3D Focused Ion Beam (FIB)/Scanning Electron Microscope (SEM) system was used to locate an isolated ANW and to fabricate Pt contacts on it. The focused ion beam etched the oxide layer and ensured good ohmic contact with the wire. The Pt contacts were joined by macroscopic Au wires to the voltage and current terminals of the DR.

4-probe transport measurements were made on an 80 nm (70 nm without the 5 nm thick oxide layer seen using TEM) ANW. The distance between the voltage electrodes for this wire was 4.8 μm. Figure 3a shows the dependence of resistance on temperature ($R(T)$) at a DC excitation current of 100 nA. The superconducting transition occurs at a critical temperature $T_c = 1.7$ K. This is higher than the T_c of bulk Al, which is 1.2 K. Transport measurements made on a 30 nm single ANW in the same configuration show an onset of superconductivity at temperature $T_c = 1.9$ K. This increase of T_c with reduction in diameter has been seen earlier in amorphous ANW synthesized using e-beam lithography[3] and in Pb nanobelts.[15] The resistivity (ρ) of the 70 nm wire in the normal state (at 4 K) is 1.07×10^{-7} Ω m which is 3.7 times the bulk resistivity and an order of magnitude larger than the resistivity of amorphous ANW of approximately the same dimensions made using electron beam lithography and evaporation.[2] The enhancement of resistivity in nanowires is generally ascribed to finite size effects, due to which the mean free path is limited to the wire diameter.

The dependence of resistance on magnetic field ($R(H)$) was measured with the magnetic field perpendicular to the sample (Figure 3b). At 0.1 K, the critical field (H_c) was 3000 Oe. This is nearly 30 times the H_c of bulk Al.

The voltage (V)−current (I) characteristics of the nanowire were also measured (Figure 3c). The critical current density (j_c) at 0.1 K was 8.7×10^4 A cm^{-2}. This is 3 orders of magnitude smaller than the bulk value of $j_c \approx 2.57 \times 10^7$ A cm^{-2} measured for aluminum strips of dimension 3.00 mm $\times$ 0.35/2.5 μm $\times$ 1.24 μm.[14] Reduction of this order in j_c from the bulk value has been seen in other single-crystal nanowires like Zn[16] and Sn[17] and hence is not unexpected. Earlier studies done on amorphous ANW have reported values of $j_c \approx 8.3 \times 10^3$ A cm^{-2} in nanowires of dimensions similar to the dimensions of the nanowires under study.[2] A possible explanation for the general trend of reduction of j_c in nanowires is the importance of fluctuations in reduced dimensionality systems.[1] Fluctuations in quasi-1D systems can weaken the superconductivity and enable small currents to completely destroy the long-range order.

In summary, single-crystal Al nanowires have been prepared for the first time by template-based electrodeposition at room temperature. XRD, HRTEM, and SAED show that the deposited ANWs are single crystal with [110] as the preferred growth direction, homogeneous diameters, and surrounding oxidation layer. Four-probe transport measurements on single nanowires have been performed. These measurements show that the superconducting properties of the nanowires are in agreement with expectations. The availability of ANWs of controllable diameters, which are surrounded by a stable, insulating oxide layer opens some exciting avenues for individual nanowire measurements on single-crystal wires, including measurements on narrower wires to study quantum phase slip phenomena and tunneling measurements to explore the superconducting state deep in the 1D regime.

(14) Romijn, J.; Klapwijk, T. M.; Renne, M. J.; Mooij, J. E. *Phys. Rev. B* **1982**, *26*, 3648.
(15) Wang, J.; Ma, X. C.; Lu, L.; Jin, A. Z.; Gu, C. Z.; Xie, X. C.; Jia, J. F.; Chen, X.; Xue, Q. K. *Appl. Phys. Lett.* **2008**, *92*, 233119.
(16) Tian, M.; Kumar, N.; Xu, S.; Wang, J.; Kurtz, J.; Chan, M. *Phys. Rev. Lett.* **2005**, *95*, 076802.
(17) Tian, M.; Wang, J.; Kurtz, J.; Liu, Y.; Chan, M.; Mayer, T.; Mallouk, T. *Phys. Rev. B* **2005**, *71*, 104521.